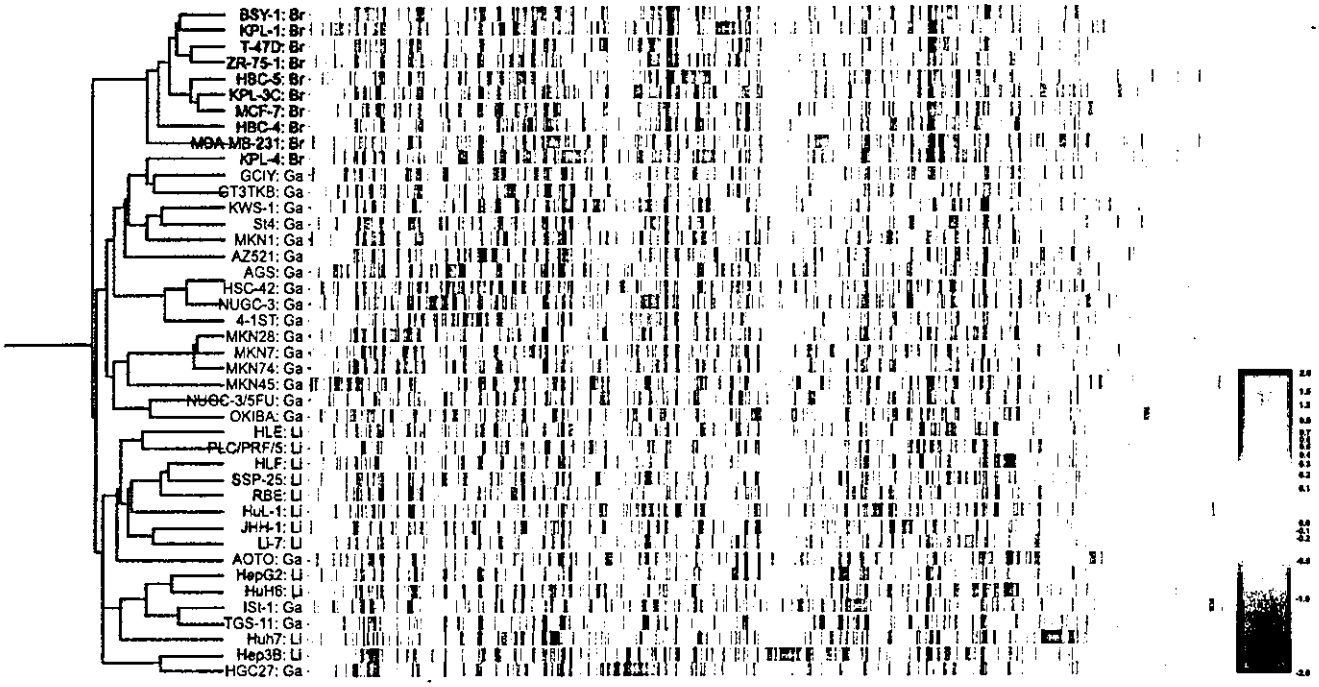

Figure 2. Hierarchical clustering of 42 human cancer cell lines based on their gene expression profiles. Gradient color indicates relative level ($\log_2$ transformed) of gene expression. *Red,* high expression of gene (2.0); *yellow,* normal expression of gene (0.0); *green,* low expression of gene (−2.0). *Red* was expressed four times more than *yellow*. *Br*, *Ga*, and *Li*, breast, stomach, and liver cancer cell lines, respectively. Cell lines with the same tissue of origin tended to form a cluster.

cancer cell lines clustered separately from the breast cancer cell lines and formed tissue-specific subclusters. However, four stomach cancer cell lines, AOTO, ISt-1, TGS-11, and HGC27, were intercalated into a cluster of liver cancer cell lines. These results suggested that the established cell lines maintained characteristics of their organ of origin as far as the gene expression profile was concerned.

Correlation Analysis between Gene Expression Profiles and Chemosensitivity Profiles

To investigate genes that may be involved in chemosensitivity, we integrated the two databases and did a correlation analysis between gene expression and drug sensitivity. Comprehensive calculations for the Pearson correlation coefficients were done on the expression of 3,537 genes and sensitivity to 53 drugs in 42 cell lines. We selected genes that satisfied the following criteria: showing a P of correlation <0.05 between the expression of the gene and its sensitivity to a certain drug and being significantly expressed in >50% of the cell lines. We examined the data for the distribution by scatter graph analysis and removed those data showing a highly non-normal distribution. The higher the expression of the gene showing positive correlation, the higher the sensitivity was to the drug (i.e., this gene was a sensitive candidate gene). In contrast, genes that showed a negative correlation with chemosensitivity were resistant candidate genes. Consequently, different sets of genes were extracted with respect to each of the 53 drugs. Table 2 shows sets of genes whose expression was correlated with the sensitivity of 42 cell lines to MMC, paclitaxel, vinorelbine, and SN-38. As for MMC, 20 genes were extracted as sensitive genes and 10 genes were extracted as resistant candidate genes. Some of these genes (such as *JUN*, *EMS1*, and *NMBR*) are related to cell growth, whereas others included various types of genes (such as *SOD1*, *PELP1*, *SFRS9*, etc.). Similarly, many sensitive and resistant candidate genes were extracted with the other drugs tested. We further applied a Pearson correlation analysis to the cell lines originating from the same organ. Genes whose expressions were correlated with the MMC sensitivity in 10 breast cancer, 12 liver cancer, and 20 stomach cancer cell lines are shown in Table 3. As described previously (19, 20), these genes may predict chemosensitivity.

Identification of Genes That Change Cellular Chemosensitivity

These genes described above may include genes that directly determine chemosensitivity. To identify such genes, we established a screening system in which we could detect any change in the anticancer drug sensitivity by monitoring cell growth inhibition. [^{3}H]thymidine incorporation was used as a variable to measure cell growth. To detect small changes in sensitivity, a higher transfection efficiency was required. Therefore, the human fibrosarcoma cell line, HT1080, which reportedly showed high transfection efficiency, was selected for the subsequent experiments. Transfection efficiency of HT1080 cells

Table 2. Genes related to the sensitivity to MMC, vinorelbine, paclitaxel, and SN-38 in 42 human cancer cell lines

Rank	Gene	Genbank ID	r	P
A. MMC				
Sensitive				
1	*SF1*	D26121	0.566	0.001
2	*CBR3*	Ab004854	0.486	0.006
3	*EMS1*	M98343	0.480	0.010
4	*JUN*	J04111	0.473	0.015
5	*SFRS9*	U30825	0.448	0.010
6	*NMBR*	M73482	0.428	0.012
7	*RBMX*	Z23064	0.419	0.012
8	*SOD1*	M13267	0.418	0.024
9	*NOL1*	X55504	0.415	0.025
10	*PELP1*	U88153	0.405	0.019
11	*ARHA*	L25080	0.404	0.030
12	*AARS*	D32050	0.398	0.018
13	*NME1*	X17620	0.398	0.032
14	*HNRPA2B1*	M29065	0.390	0.044
15	*NME2*	L16785	0.378	0.025
16	*VAT1*	U18009	0.376	0.031
17	*SERPINB10*	U35459	0.372	0.028
18	*KIAA0436*	AB007896	0.353	0.041
19	*DRPLA*	D31840	0.350	0.049
20	*MC3R*	L06155	0.346	0.049
Resistant				
1	*SPTBN1*	M96803	−0.450	0.013
2	*PET112L*	AF026851	−0.425	0.027
3	*CAPN1*	X04366	−0.421	0.032
4	*MEL*	X56741	−0.414	0.028
5	*PACE*	X17094	−0.380	0.035
6	*DVL2*	AF006012	−0.370	0.034
7	*LOC54543*	AJ011007	−0.366	0.022
8	*PAPOLA*	X76770	−0.351	0.033
9	*RPLP2*	M17887	−0.345	0.049
10	*ARF4L*	L38490	−0.340	0.042
B. Vinorelbine				
Sensitive				
1	*ARHA*	L25080	0.534	0.003
2	*NME2*	L16785	0.521	0.001
3	*VIL2*	X51521	0.463	0.015
4	*YWHAQ*	X56468	0.450	0.011
5	*HK1*	M75126	0.449	0.016
6	*SATB1*	M97287	0.439	0.006
7	*CAMLG*	U18242	0.439	0.007
8	*CARS*	L06845	0.433	0.007
9	*CCNB1*	M25753	0.427	0.013
10	*U2AF1*	M96982	0.424	0.022
11	*PTMA*	M26708	0.423	0.018
12	*MLC1SA*	M31211	0.397	0.022
13	*NME1*	X17620	0.393	0.035
14	*SARS*	X91257	0.386	0.032
15	*CDC20*	U05340	0.385	0.029
16	*PPP4C*	X70218	0.385	0.039
17	*TNFAIP3*	M59465	0.384	0.023
18	*EEF1D*	Z21507	0.384	0.023
19	*PFKP*	D25328	0.365	0.028
20	*ENTPD2*	U91510	0.365	0.037
21	*CCL5*	M21121	0.358	0.035
22	*ACAT1*	D90228	0.352	0.048
23	*IQGAP1*	L33075	0.351	0.042
24	*PAX5*	M96944	0.342	0.038
25	*NRGN*	Y09689	0.336	0.042
26	*K-α-1*	K00558	0.328	0.048
27	*NDUFB7*	M33374	0.321	0.049
Resistant				
1	*HOXB1*	X16666	−0.600	0.000
2	*F10*	K03194	−0.514	0.002
3	*GPX2*	X53463	−0.509	0.002
4	*NR1I2*	AF061056	−0.498	0.002
5	*ANXA4*	M19383	−0.481	0.005
6	*PDLIM1*	U90878	−0.465	0.006
7	*LIPC*	X07228	−0.464	0.004
8	*SERPINF2*	D00174	−0.447	0.004
9	*HSD17B1*	M36263	−0.443	0.014
10	*MAN2B1*	U60266	−0.440	0.008
11	*LSS*	D63807	−0.430	0.014
12	*PIK3CG*	X83368	−0.415	0.010
13	*DBN1*	U00802	−0.414	0.017
14	*NDUFA4*	U94586	−0.410	0.038
15	*BDH*	M93107	−0.399	0.024
16	*BCL2L1*	Z23115	−0.385	0.039
17	*EEF1B2*	X60656	−0.383	0.030
18	*F2*	V00595	−0.382	0.026
19	*RARA*	X06614	−0.369	0.029
20	*ITGB4*	X53587	−0.367	0.042
21	*IMPA1*	X66922	−0.367	0.042
22	*PACE*	X17094	−0.367	0.042
23	*AGA*	M64073	−0.361	0.042
24	*MVD*	U49260	−0.353	0.038
25	*EHHADH*	L07077	−0.346	0.039
26	*TFPI2*	D29992	−0.343	0.035
27	*MARCKS*	M68956	−0.342	0.045
28	*FGB*	J00129	−0.334	0.035
29	*GPD1*	L34041	−0.322	0.049
C. Paclitaxel				
Sensitive				
1	*ADH6*	M68895	0.513	0.002
2	*RAB28*	X94703	0.480	0.007
3	*U2AF1*	M96982	0.441	0.017
4	*GPC1*	X54232	0.440	0.013
5	*HK1*	M75126	0.439	0.020
6	*CARS*	L06845	0.436	0.006
7	*TNFAIP3*	M59465	0.433	0.009
8	*K-α-1*	K00558	0.418	0.010
9	*PFKP*	D25328	0.416	0.012
10	*GDI2*	D13988	0.411	0.033
11	*VIL2*	X51521	0.410	0.034
12	*RUNX2*	AF001450	0.409	0.038
13	*NME2*	L16785	0.407	0.015
14	*CDC20*	U05340	0.395	0.025
15	*GNAI2*	X04828	0.391	0.033

NOTE: Column 2 shows the name of the gene according to HUGO database. Column 4 shows Pearson correlation coefficient between chemosensitivity to drugs and gene expression. "Sensitive" indicates candidate genes sensitive to each drug. "Resistant" indicates genes resistant to each drug.

(Continued on the following page)

Table 2. Genes related to the sensitivity to MMC, vinorelbine, paclitaxel, and SN-38 in 42 human cancer cell lines (Cont'd)

Rank	Gene	Genbank ID	r	P
16	*ARHA*	L25080	0.381	0.041
17	*CNR2*	X74328	0.378	0.030
18	*PPP2R2B*	M64930	0.376	0.026
19	*SLC6A8*	L31409	0.374	0.046
20	*DDX9*	L13848	0.374	0.042
21	*ACAT1*	D90228	0.369	0.038
22	*PI3*	Z18538	0.329	0.047
Resistant				
1	*NAP1L1*	M86667	−0.530	0.004
2	*HOXB1*	X16666	−0.516	0.004
3	*PACE*	X17094	−0.507	0.004
4	*MAN2B1*	U60266	−0.486	0.003
5	*GPX2*	X53463	−0.480	0.004
6	*DBN1*	U00802	−0.469	0.006
7	*ANXA4*	M19383	−0.468	0.007
8	*SERPINF2*	D00174	−0.463	0.003
9	*AGA*	M64073	−0.444	0.011
10	*BCL2L1*	Z23115	−0.428	0.021
11	*LIPC*	X07228	−0.401	0.015
12	*BDH*	M93107	−0.393	0.026
13	*LSS*	D63807	−0.384	0.030
14	*PDLIM1*	U90878	−0.372	0.033
15	*ZNF161*	D28118	−0.368	0.038
16	*UBE2E1*	X92963	−0.363	0.032
17	*TLE1*	M99435	−0.360	0.039
18	*RARA*	X06614	−0.359	0.034
19	*PTPRN*	L18983	−0.357	0.035
20	*APOE*	M12529	−0.353	0.048
21	*F10*	K03194	−0.348	0.040
22	*NR1I2*	AF061056	−0.342	0.041
23	*UBE2L3*	X92962	−0.332	0.045
24	*FGB*	J00129	−0.313	0.049
D. SN-38				
Sensitive				
1	*EMS1*	M98343	0.573	0.001
2	*JUN*	J04111	0.564	0.003
3	*IL-6*	X04602	0.514	0.003
4	*RPL23*	X52839	0.495	0.004
5	*CDKN3*	L25876	0.455	0.017
6	*RPL3*	X73460	0.445	0.011
7	*TFPI*	J03225	0.442	0.009
8	*MRPL3*	X06323	0.437	0.009
9	*HLA-C*	M11886	0.424	0.014
10	*AARS*	D32050	0.419	0.012
11	*ARHGDIA*	X69550	0.416	0.031
12	*NOL1*	X55504	0.406	0.029
13	*SF1*	D26121	0.394	0.031
14	*SOD1*	M13267	0.389	0.037
15	*VEGF*	M32977	0.384	0.043
16	*EIF2S1*	J02645	0.382	0.034
17	*CDH5*	X79981	0.372	0.030
18	*FOSL1*	X16707	0.371	0.047
19	*IDS*	M58342	0.366	0.047
20	*PMVK*	L77213	0.364	0.044
21	*PPP2CB*	X12656	0.364	0.041
22	*NMBR*	M73482	0.362	0.035
23	*RPL26*	X69392	0.358	0.035
24	*PELP1*	U88153	0.356	0.042
25	*MC3R*	L06155	0.356	0.042
26	*RPS8*	X67247	0.355	0.036
Resistant				
1	*CAPN1*	X04366	−0.496	0.010
2	*MEL*	X56741	−0.478	0.010
3	*PACE*	X17094	−0.443	0.012
4	*TIMP2*	J05593	−0.433	0.019
5	*AOP2*	D14662	−0.422	0.025
6	*ZNF174*	U31248	−0.402	0.018
7	*ID3*	X69111	−0.393	0.038
8	*KLF5*	D14520	−0.384	0.036
9	*CALD1*	M64110	−0.382	0.031
10	*LOC54543*	AJ011007	−0.368	0.021
11	*PTPN3*	M64572	−0.363	0.038
12	*ACTB*	X00351	−0.362	0.025
13	*LY6E*	U42376	−0.360	0.037
14	*ID1*	D13889	−0.343	0.044

(Continued)

was >90% as evaluated by transfection of a plasmid expressing the enhanced green fluorescent protein (data not shown). To validate this screening system, we examined the effect of *NQO1* gene, coding DT-diaphorase that increases cellular sensitivity to MMC (12). As shown in Fig. 3B, cells transfected with NQO1 significantly enhanced growth inhibition by MMC compared with the mock-transfected and LacZ-transfected cells. We confirmed the cellular expression of the *NQO1* gene product by immunoblot (Fig. 3C). Thus, this screening system can be used to detect changes in chemosensitivity in HT1080 cells. Using this screening system, we examined whether the 19 genes, which were extracted in Tables 2 and 3, altered sensitivity to drug. Notably, the *HSPA1A* gene coding 70-kDa heat shock protein, whose expression was correlated with MMC sensitivity in the breast and liver cancer cell lines, significantly enhanced the MMC sensitivity in HSPA1A-transfected HT1080 cells (Fig. 3B). Similarly, the *JUN* gene encoding c-JUN, whose expression was correlated with MMC sensitivity, also enhanced the MMC sensitivity in JUN-transfected HT1080 cells (Fig. 3B). The expression of *myc*-tagged LacZ, 70-kDa heat shock protein, and JUN in the transfected cells was confirmed by immunoblotting with anti-*myc* antibody (Fig. 3C). Transfection with 17 other genes did not alter the MMC sensitivity. For example, transfection with the *IL-18* gene did not affect MMC sensitivity (Fig. 3B).

Discussion

The assessment system for determining pharmacologic properties of chemicals by a panel of cancer cell lines was first developed in the National Cancer Institute (33–35). We established a similar assessment system (JFCR-39;

Table 3. Genes related to MMC sensitivity in breast, liver, and stomach cancer cell lines

Rank	Gene	Genbank ID	*r*	*P*
A. Breast cancer				
Sensitive				
1	*INHBB*	M31682	0.972	0.000
2	*NK4*	M59807	0.838	0.018
3	*HSPA1A*	M11717	0.751	0.050
4	*LOC54557*	AF075050	0.735	0.024
5	*CD47*	Y00815	0.717	0.045
Resistant				
1	*RPN2*	Y00282	−0.882	0.009
2	*ATP5O*	X83218	−0.842	0.017
3	*CAST*	D50827	−0.815	0.025
4	*HPCA*	D16593	−0.776	0.024
5	*ZNF9*	M28372	−0.774	0.024
6	*A2LP*	U70671	−0.772	0.042
7	*IL-18*	D49950	−0.747	0.033
8	*NRGN*	Y09689	−0.727	0.041
B. Liver cancer				
Sensitive				
1	*EB1*	U24166	0.872	0.002
2	*JUN*	J04111	0.813	0.008
3	*EIF3S8*	U46025	0.772	0.015
4	*CTSD*	M11233	0.753	0.012
5	*SCYA5*	M21121	0.741	0.022
6	*PHB*	S85655	0.739	0.023
7	*HSPA1A*	M11717	0.729	0.026
8	*SPP1*	X13694	0.723	0.018
9	*TAB7*	X93499	0.712	0.021
10	*ACTN1*	X15804	0.692	0.039
11	*RXRB*	M84820	0.678	0.045
12	*PSME2*	D45248	0.673	0.047
13	*HLA-C*	M11886	0.647	0.043
14	*RPL19*	X63527	0.643	0.033
Resistant				
1	*MAPK6*	X80692	−0.862	0.003
2	*GCSH*	M69175	−0.793	0.006
3	*G22P1*	M32865	−0.727	0.017
4	*USP11*	U44839	−0.725	0.027
5	*ACTB*	X00351	−0.715	0.020
6	*YWHAZ*	M86400	−0.706	0.022
7	*IL-10*	M57627	−0.694	0.018
8	*RFC4*	M87339	−0.677	0.016
9	*CRLF1*	AF059293	−0.644	0.033
10	*RPS6*	M20020	−0.619	0.042
11	*EMX1*	X68879	−0.618	0.043
12	*TK2*	U77088	−0.607	0.047
C. Stomach cancer				
Sensitive				
1	*TEAD4*	U63824	0.803	0.001
2	*NR2C2*	U10990	0.713	0.001
3	*CSF1*	M37435	0.711	0.004
4	*RAB28*	X94703	0.695	0.008
5	*CBR3*	Ab004854	0.683	0.007
6	*NFYC*	Z74792	0.639	0.019
7	*PGF*	X54936	0.627	0.022
8	*ERG*	M21535	0.620	0.005
9	*MLLT1*	L04285	0.613	0.015
10	*FOS*	K00650	0.599	0.014
11	*TNFAIP3*	M59465	0.584	0.011
12	*CNR2*	X74328	0.581	0.009
13	*DRPLA*	D31840	0.577	0.024
14	*PSMB5*	D29011	0.572	0.026
15	*SLC6A8*	L31409	0.570	0.017
16	*SERPINB10*	U35459	0.570	0.013
17	*VAT1*	U18009	0.570	0.009
18	*TJP1*	L14837	0.562	0.029
19	*PELP1*	U88153	0.545	0.035
20	*C1QBP*	L04636	0.545	0.024
21	*CDK10*	L33264	0.543	0.045
22	*SERPINA6*	J02943	0.542	0.025
23	*ACTB*	X00351	0.538	0.021
24	*SFRP4*	AF026692	0.538	0.018
25	*EMX1*	X68879	0.535	0.018
26	*ACTB*	X00351	0.529	0.024
27	*RPS9*	U14971	0.528	0.043
28	*AMD1*	M21154	0.522	0.038
29	*RPL26*	X69392	0.522	0.038
30	*HNRPF*	L28010	0.520	0.047
31	*PTMS*	M24398	0.502	0.040
32	*STK12*	AF008552	0.498	0.050
33	*NR2F6*	X12794	0.491	0.046
34	*GBE1*	L07956	0.470	0.049
Resistant				
1	*PSMD8*	D38047	−0.747	0.002
2	*LAMP2*	J04183	−0.677	0.002
3	*CTSD*	M11233	−0.651	0.006
4	*ADORA2B*	M97759	−0.645	0.005
5	*ANXA4*	M19383	−0.639	0.008
6	*PTPRK*	Z70660	−0.638	0.003
7	*RAD23A*	D21235	−0.622	0.010
8	*SDHA*	D30648	−0.613	0.015
9	*PET112L*	AF026851	−0.598	0.024
10	*DAD1*	D15057	−0.593	0.025
11	*HSPB1*	X54079	−0.588	0.013
12	*PSMA6*	X61972	−0.586	0.036
13	*KDELR1*	X55885	−0.584	0.028
14	*B2M*	AB021288	−0.581	0.023
15	*M6PR*	M16985	−0.579	0.038
16	*GCLC*	M90656	−0.576	0.015
17	*SPTBN1*	M96803	−0.557	0.038
18	*PACE*	X17094	−0.547	0.019
19	*RPL24*	M94314	−0.539	0.017
20	*SPINT2*	U78095	−0.538	0.039
21	*STX4A*	U07158	−0.534	0.027
22	*SIAT8B*	U33551	−0.532	0.028
23	*CTSK*	U13665	−0.529	0.029
24	*DCI*	L24774	−0.525	0.044
25	*MEL*	X56741	−0.525	0.045
26	*PITPNB*	D30037	−0.523	0.038
27	*YY1*	M76541	−0.512	0.043
28	*RAB1*	M28209	−0.495	0.037
29	*UBE2L6*	AF031141	−0.492	0.045
30	*PSMB7*	D38048	−0.484	0.049

NOTE: Column 2 shows the name of the gene according to HUGO database. Column 4 shows Pearson correlation coefficient between chemosensitivity to drugs and gene expression. "Sensitive" indicates candidate genes sensitive to each drug. "Resistant" indicates genes resistant to each drug.

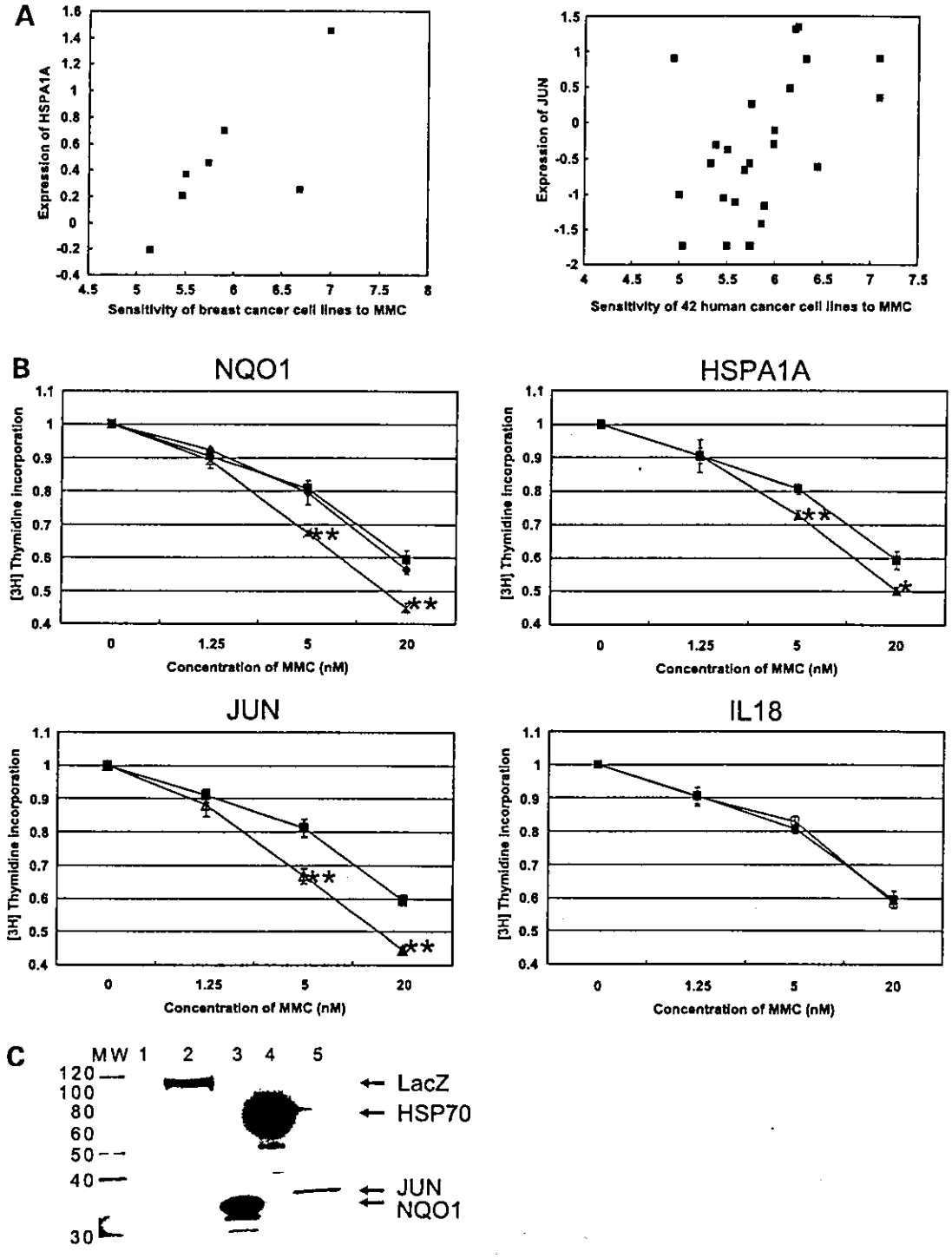

Figure 3. Relationships between MMC sensitivity and expression of HSPA1A in breast cancer cell lines (**A**, *left*) or JUN in 42 cell lines (**A**, *right*). Each symbol indicates one cell line. *X axis*, MMC sensitivity; *Y axis*, expression of HSPA1A or JUN. Pearson correlation coefficients between MMC sensitivity and expression of HSPA1A and JUN were 0.75 ($P \approx 0.05$) and 0.473 ($P = 0.015$), respectively. **B**, growth inhibition curves by MMC in mock (■), LacZ (♦), NQO1 (×), HSPA1A (▲), JUN (△), or IL-18 (□) transfected HT1080 cells. This growth inhibition by MMC was enhanced in HT1080 cells transfected with NQO1, HSPA1A, and JUN. *, $P < 0.002$; **, $P < 0.0001$, *t* test against mock-transfected cells. **C**, expressions of genes were certified by immunoblotting with anti-*myc* antibody: *myc*-tagged LacZ (*lane 2*), NQO1 (*lane 3*), 70-kDa heat shock protein (*HSP70*; *lane 4*), and JUN (*lane 5*).

ref. 32) and showed that drugs with similar modes of actions were classified into the same cluster by hierarchical clustering (19). In this study, we constructed a new panel of 45 human cancer cell lines (JFCR-45), comprising cancer cell lines derived from tumors from three different organ types: breast, liver, and stomach. In particular, the inclusion of cell lines derived from gastric and hepatic cancers is a major point of novelty. JFCR-45 can be used for analyzing both organ-specific differences in chemosensitivity and intraorgan heterogeneity of chemosensitivity. We examined 53 anticancer drugs for their activity against JFCR-45 and observed differential activity across the whole panel as well as within a single organ type (e.g., breast, liver, or stomach). Furthermore, as shown in Fig. 1, using JFCR-45, drugs with a similar mode of action (such as a tubulin binder or topo I inhibitor) were classified into the same cluster, which were the same as the clusters established for NCI-60 (35) and JFCR-39 (19). These results suggest that the cell line panel-based assessment system is generally effective for classifying anticancer drugs with the same modes of action into the same set of clusters.

In this study, we investigated the gene expression profiles of 42 cell lines of JFCR-45 using cDNA array consisting of 3,537 genes. Hierarchical clustering analysis of these gene expression profiles classified organ-specific cell lines mostly into the same cluster, suggesting that these cell lines maintained the genetic characteristics of the parent organ as far as the gene expression profiles were concerned.

We did a Pearson correlation analysis of the gene expression database and the drug sensitivity database. Consequently, many genes whose expressions were correlated with respect to the sensitivity of each drug were identified. For example, DNA alkylating agents and nucleic acid–related genes, including *SF1* encoding ZFM1, *c-JUN* oncogene, and *SFRS9* were extracted as the genes sensitive to MMC. The genes that were sensitive to paclitaxel included tubulin binder and cytoskeleton-related genes, such as *VIL2* encoding ezrin and *ACTB* encoding β-actin.

These results suggest that the extracted genes are the predictive markers of drug efficacy. We further applied Pearson correlation analysis to each type (i.e., breast, liver, or stomach cancer) of cell lines. There were two advantages in this type of analysis: one is that we could compare the cell lines having the same organ background and another is that organ-specific genes, which worked as the sensitive or resistant factors, could be extracted. For example, for MMC, several genes (such as *INHBB*, *NK4*, and *HSPA1A*) were newly extracted as candidate genes sensitive to MMC from the breast cancer cell lines. Surprisingly, compared with the breast and liver cancer cells, many new candidate genes were extracted from the stomach cancer cell lines. These extracted genes were considered as the candidates for organ-specific predictive markers of drug efficacy.

We hypothesized that some of the candidate sensitivity genes described above might causally affect the chemosensitivity of cancer cell lines. To validate this possibility, we selected 19 genes, including *HSPA1A*, *JUN*, and *IL-18*, and examined whether the expression of these candidate genes would affect the cellular sensitivity to anticancer drugs. Overexpression of 2 of the 19 genes, *HSPA1A* encoding 70-kDa heat shock protein and *JUN* encoding c-JUN, indeed enhanced cellular sensitivity to MMC in HT1080 cells (Fig. 3), suggesting that they function to mediate MMC sensitivity. This was an unexpected finding, because a direct relationship between these two genes and MMC sensitivity has not been reported previously, although a relationship between heat shock protein and cancer has been suggested previously (36, 37). How these two genes potentiate MMC sensitivity remains to be clarified. In this validation, we used the HT1080 cell line instead of those in JFCR-45 because of its high transfection efficiency. As the alteration of chemosensitivity following the overexpression of any particular gene may depend highly on the genotypic/phenotypic background of the transfected HT1080 cells, further validation using cell lines within JFCR-45 will be required. In addition to the overexpression experiments, validation by silencing chemosensitivity-related genes using small interfering RNA will be required.

Pioneering attempts to discover new leads and targets and to investigate new aspects of the molecular pharmacology of anticancer drugs by mining the NCI-60 database have been done (31, 33-35). Recently, Szakacs et al. (38) have identified interesting compounds whose activity is potentiated by the MDR1 multidrug transporter. Our previous studies using JFCR-39 (19, 20, 31) and the present study using JFCR-45 also indicate that a comprehensive analysis of chemosensitivity and gene expression data followed by experimental validation leads to the identification of genes that determine drug sensitivity.

In conclusion, we established a sensitivity database for JFCR-45, which focused on organ origin, to 53 anticancer drugs. Using JFCR-45, anticancer drugs were classified according to their modes of action. Moreover, we established a database of the gene expression profiles in 42 cell lines of JFCR-45. Using these two databases, we have identified several genes that may predict chemosensitivity of cancer. Among these candidate genes, we identified two genes, *HSPA1A* and *JUN*, which determined sensitivity to MMC. Thus, this approach is useful not only to discover predictive markers for the efficacy of anticancer drugs but also to discover genes that determine chemosensitivity.

Acknowledgments

We thank Yumiko Mukai, Yumiko Nishimura, Mariko Seki, and Fujiko Ohashi for the determination of chemosensitivity and Dr. Munetika Enjoji (Department of Internal Medicine, National Kyushu Cancer Center, Fukuoka, Japan) for providing the RBE and SSP-25 cell lines.

References

1. Chen CJ, Clark D, Ueda K, et al. Genomic organization of the human multidrug resistance (MDR1) gene and origin of P-glycoproteins. J Biol Chem 1990;265:506–14.

2. Taniguchi K, Wada M, Kohno K, et al. A human canalicular multispecific organic anion transporter (cMOAT) gene is overexpressed in cisplatin-resistant human cancer cell lines with decreased drug accumulation. Cancer Res 1996;56:4124–9.

3. Kool M, de Haas M, Scheffer GL, et al. Analysis of expression of cMOAT (MRP2), MRP3, MRP4, and MRP5, homologues of the multidrug

resistance-associated protein gene (MRP1), in human cancer cell lines. Cancer Res 1997;57:3537–47.

4. Patterson LH, Murray GI. Tumour cytochrome *P*450 and drug activation. Curr Pharm Des 2002;8:1335–47.

5. Batist G, Tulpule A, Sinha BK, et al. Overexpression of a novel anionic glutathione transferase in multidrug-resistant human breast cancer cells. J Biol Chem 1986;261:15544–9.

6. Meisel P. Arylamine *N*-acetyltransferases and drug response. Pharmacogenomics 2002;3:349–66.

7. Nair MG, Baugh CM. Synthesis and biological evaluation of poly-γ-glutamyl derivatives of methotrexate. Biochemistry 1973;12:3923–7.

8. Schimke RT. Methotrexate resistance and gene amplification. Mechanisms and implications. Cancer 1986;57:1912–7.

9. Pinedo HM, Peters GF. Fluorouracil: biochemistry and pharmacology. J Clin Oncol 1988;6:1653–64.

10. Eastman A. Mechanisms of resistance to cisplatin. Cancer Treat Res 1991;57:233–49.

11. Cohen SS. The mechanisms of lethal action of arabinosyl cytosine (araC) and arabinosyl adenine (araA). Cancer 1977;40:509–18.

12. Gustafson DL, Pritsos CA. Enhancement of xanthine dehydrogenase mediated mitomycin C metabolism by dicumarol. Cancer Res 1992;52:6936–9.

13. Kang HC, Kim IJ, Park JH, et al. Identification of genes with differential expression in acquired drug-resistant gastric cancer cells using high-density oligonucleotide microarrays. Clin Cancer Res 2004;10:272–84.

14. Sato T, Odagiri H, Ikenaga SK, et al. Chemosensitivity of human pancreatic carcinoma cells is enhanced by IκBα super-repressor. Cancer Sci 2003;94:467–72.

15. Zembutsu H, Ohnishi Y, Tsunoda T, et al. Genome-wide cDNA microarray screening to correlate gene expression profiles with sensitivity of 85 human cancer xenografts to anticancer drugs. Cancer Res 2002;62:518–27.

16. Okutsu J, Tsunoda T, Kaneta Y, et al. Prediction of chemosensitivity for patients with acute myeloid leukemia, according to expression levels of 28 genes selected by genome-wide complementary DNA microarray analysis. Mol Cancer Ther 2002;1:1035–42.

17. Tanaka T, Tanimoto K, Otani K, et al. Concise prediction models of anticancer efficacy of 8 drugs using expression data from 12 selected genes. Int J Cancer 2004;111:617–26.

18. Scherf U, Ross DT, Waltham M, et al. A gene expression database for the molecular pharmacology of cancer. Nat Genet 2000;24:236–44.

19. Dan S, Tsunoda T, Kitahara O, et al. An integrated database of chemosensitivity to 55 anticancer drugs and gene expression profiles of 39 human cancer cell lines. Cancer Res 2002;62:1139–47.

20. Dan S, Shirakawa M, Mukai Y, et al. Identification of candidate predictive markers of anticancer drug sensitivity using a panel of human cancer cell lines. Cancer Sci 2003;94:1074–82.

21. Kurebayashi J, Kurosumi M, Sonoo H. A new human breast cancer cell line, KPL-3C, secretes parathyroid hormone-related protein and produces tumours associated with microcalcifications in nude mice. Br J Cancer 1996;74:200–7.

22. Shiu RP. Processing of prolactin by human breast cancer cells in long term tissue culture. J Biol Chem 1980;255:4278–81.

23. Engel LW, Young NA, Tralka TS, et al. Establishment and characterization of three new continuous cell lines derived from human breast carcinomas. Cancer Res 1978;38:3352–64.

24. Dor I, Namba M, Sato J. Establishment and some biological characteristics of human hepatoma cell lines. Gann 1975;66:385–92.

25. Tanaka M, Kawamura K, Fang M, et al. Production of fibronectin by HUH6 C15 cell line established from a human hepatoblastoma. Biochem Biophys Res Commun 1983;110:837–41.

26. Fukutomi M, Enjoji M, Iguchi H, et al. Telomerase activity is repressed during differentiation along the hepatocytic and biliary epithelial lineages: verification on immortal cell lines from the same origin. Cell Biochem Funct 2001;19:65–8.

27. Sorimachi K, Hayashi T, Takaoka T, et al. Requirement of serum pretreatment for induction of alkaline phosphatase activity with prednisolone, butyrate, dibutyryl cyclic adenosine monophosphate and NaCl in human liver cells continuously cultured in serum-free medium. Cell Struct Funct 1988;13:1–11.

28. Fujise K, Nagamori S, Hasumura S, et al. Integration of hepatitis B virus DNA into cells of six established human hepatocellular carcinoma cell lines. Hepatogastroenterology 1990;37:457–60.

29. Imanishi K, Yamaguchi K, Suzuki M, et al. Production of transforming growth factor-α in human tumour cell lines. Br J Cancer 1989;59:761–5.

30. Yamori T, Matsunaga A, Sato S, et al. Potent antitumor activity of MS-247, a novel DNA minor groove binder, evaluated by an *in vitro* and *in vivo* human cancer cell line panel. Cancer Res 1999;59:4042–9.

31. Monks A, Scudiero D, Skehan P, et al. Feasibility of a high-flux anticancer drug screen using a diverse panel of cultured human tumor cell lines. J Natl Cancer Inst 1991;83:757–66.

32. Yamori T. Panel of human cancer cell lines provides valuable database for drug discovery and bioinformatics. Cancer Chemother Pharmacol 2003;52 Suppl 1:S74–9.

33. Paull KD, Shoemaker RH, Hodes L, et al. Display and analysis of patterns of differential activity of drugs against human tumor cell lines: development of mean graph and COMPARE algorithm. J Natl Cancer Inst 1989;81:1088–92.

34. Weinstein JN, Kohn KW, Grever MR, et al. Neural computing in cancer drug development: predicting mechanism of action. Science 1992;258:447–51.

35. Weinstein JN, Myers TG, O'Connor PM, et al. An information-intensive approach to the molecular pharmacology of cancer. Science 1997;275:343–9.

36. Laroia G, Cuesta R, Brewer G, et al. Control of mRNA decay by heat shock-ubiquitin-proteasome pathway. Science 1999;284:499–502.

37. Jolly C, Morimoto RI. Role of the heat shock response and molecular chaperones in oncogenesis and cell death. J Natl Cancer Inst 2000;92:1564–72.

38. Szakacs G, Annereau JP, Lababidi S, et al. Predicting drug sensitivity and resistance: profiling ABC transporter genes in cancer cells. Cancer Cell 2004;6:129–37.

INT. J. RADIAT. BIOL., SEPTEMBER, 2004, VOL. 80, NO. 9, 673–681

Taylor & Francis
healthsciences

Cytological basis for enhancement of radiation-induced mortality by Friend leukaemia virus infection

K. TANAKA†, K. WATANABE†, S. YAMAGUCHI‡, M. HASEGAWA‡, M. KITAGAWA‡ and S. AIZAWA†*

(Received 24 March 2003; accepted 30 July 2004)

Abstract.
Purpose: To analyse the cytological basis for enhancement of radiation-induced mortality by Friend leukaemia virus infection.
Materials and methods: Cellularity in haematopoietic tissues of C3H mice infected with FLV and/or whole-body irradiation was examined.
Results: When mice were treated with a sublethal dose (3 Gy) of irradiation at 1 week after virus infection, most manifested a severe loss of cellularity in the spleen, bone marrow and peripheral blood 2 weeks after irradiation. More than 90% of the mice died within 1 month post-irradiation. However, this deleterious effect of virus infection on the survival of irradiated mice was observed only when they were irradiated at around 1 week after virus inoculation. Strain differences in the sensitivity to this effect were observed among virus-sensitive strains of mice.
Conclusions: The results indicate that Friend leukaemia virus infection can cause enhancement of radiation sensitivity of haematopoietic cells in host animals in a restricted manner in terms of genetic background and the interval between infection and irradiation.

1. Introduction

Exposure of animals to ionizing radiation causes physiological changes that, depending on the exposure dose, lead to death by haematopoietic and/or intestinal damage. Although it is generally accepted that radiation sensitivity is primarily determined by the intrinsic property of radiosensitivity and the initial number of stem cells (Korn and Kallman 1956, Yuhas and Storer 1962, Van Bekkum 1991, Mori *et al.* 1994), it can also be influenced by epigenetic factors. For example, it is known that microbial infection is an important factor in death associated with radiation, and that it can be controlled to some extent by treatment with antibiotics (Miller *et al.* 1950, Bennet *et al.* 1951). The critical role of bacterial infection in intestinal and haematological radiation deaths has been confirmed by the fact that the germ-free state provides increased radioresistance measured by survival (McLaughlin *et al.* 1964).

It has been recognized that living organisms are exposed to numerous natural and man-made agents that interact with molecules, cells and tissues, and that the combined exposures to radiation and other environmental factors must be taken into account when conducting risk assessments (UNSCEAR 1982, 2000). Viruses are one of the common environmental factors for humans. However, the combined effect of virus infection with radiation has been less well understood. Recently, the relationship of virus infection with the induction of apoptosis has become a topic of interest, since human immunodeficiency virus (HIV) infection is believed to kill cells in patients at least partly by an apoptotic mechanism (Corbeil and Richman 1995, Accornero *et al.* 1998). On the other hand, it has been reported that some viruses have incorporated genes that encode anti-apoptotic proteins or modulate the expression of cellular regulators of apoptosis, although the induction of apoptosis of virus-infected cells is an important host cell defence mechanism (Meinl *et al.* 1998).

The Friend leukaemia virus (FLV) is a murine retrovirus that can cause splenomegaly and induce erythroleukaemia in susceptible mice. FLV infection usually causes anti-apoptotic features in transformed cell lines (Kelly *et al.* 1998, Pereira *et al.* 1999, Quang *et al.* 1999). On the other hand, Shen *et al.* (1988) reported a curative effect of split low-dosage total-body irradiation on FLV-induced leukaemogenesis in DBA mice, suggesting that a decrease in the number of immunosuppressive $CD8^+$ T-cells may be related to the curative effect of irradiation. However, Kitagawa *et al.* (2002) observed a contradictory effect of FLV infection on survival of another FLV-susceptible strain, C3H mice, namely that FLV infection strongly enhances radiation-induced mortality of C3H mice. Therefore, virus infection might affect radiation in different ways.

The present study further characterized the effect

*Author for correspondence; e-mail: e-mail: aizawa@nirs.go.jp
†Radiation Hazards Research Group, National Institute of Radiological Sciences, 4-9-1, Anagawa, Inage, Chiba 263-8555, Japan.
‡Department of Pathology and Immunology, Aging and Developmental Sciences, Tokyo Medical and Dental University, Graduate School, Tokyo 113-8519, Japan.

International Journal of Radiation Biology ISSN 0955-3002 print/ISSN 1362-3095 online © 2004 Taylor & Francis Ltd
http://www.tandf.co.uk/journals
DOI: 10.1080/09553000400005502

of virus infection as a modification factor on radiation-induced mortality. The results indicated that the enhancing effect of FLV infection observed was manifested in a restricted manner in terms of genetic background and the interval between infection and irradiation.

2. Materials and methods

2.1. *Mice*

C3H/HeMsNrs (C3H, H-2^k, Fv-2^s), B10/Sn (B10, H-2^b, Fv-2^r) and BALB/c-Fv-4^r (C4W, H-2^d, Fv-4^r) male mice, produced in the present authors' own colonies at the Animal Production Facility of their Institute, were used at 10–15 weeks of age throughout the study. DBA/2Cr Slc (DBA/2, H-2^d, Fv-2^s) and CBA/N Slc (CBA/N, H-2^k, Fv-2^s) mice were purchased from Shizuoka Laboratory Animal Cooperation (Shizuoka, Japan). All mice were maintained in a microbiologically clean animal facility. Experiments were performed with the approval of the local committee on animal experiments, established by the National Institute of Radiological Sciences according to the Japanese Law for Handling of Experimental Animals.

2.2. *Virus infection and total-body irradiation (TBI)*

NB-tropic, polycythemic FLV complex, originally a gift from Dr C. Friend, was prepared as described by Kitagawa *et al.* (1986) and inoculated intraperitoneally (i.p.) at a highly leukaemogenic dose of 10^4 PFU/mouse (Kitagawa *et al.* 1999). Mice were then exposed to X-rays with a Pantak X-ray generator (Shimadzu Ltd, Kyoto, Japan) at a dose-rate of 0.7 Gy min^{-1} (irradiation parameters: 200 kVp, 20 mA, 0.5 mm Cu/0.5 mm Al filters) with graded doses (0.5–3.0 Gy) and at various time intervals (3–21 days) after virus inoculation. Mice were whole-body irradiated. Sham-irradiated mice, i.e. not irradiated, were also similarly prepared in each experiment.

2.3. *Measurement of cellularity*

Cellularity of bone marrow and spleen cells was analysed by flow cytometry. Briefly, spleen cells were stained with fluorescein isothiocyanate (FITC)-labelled anti-B220 monoclonal Ab and phycoerythrin (PE)-labelled anti-Thy1.2 monoclonal Ab, and bone marrow cells with FITC-labelled anti-Gr-1 monoclonal Ab and PE-labelled anti-TER119 monoclonal Ab, followed by flow cytometric analysis with FACScan (Becton Dickinson, San Jose, CA, USA) and then data analysis with CELLQuest software. All antibodies were from PharMingen (San Diego, CA, USA). Cell contents in peripheral blood were assessed using the blood cell counter Sysmex K-4500 (Toa Medical Electronics Co. Ltd, Japan).

2.4. *Measurement of haematopoietic stem cells*

The number of multipotent haematopoietic stem cells (spleen colony-forming unit; CFU-S) was examined according to the method of Till and McCulloch (1961). Either 0.5×10^5 or 1.0×10^6 donor bone marrow cells from C3H mice, treated either with FLV inoculation alone or with FLV inoculation followed by irradiation, were injected intravenously into C3H mice that had been irradiated with 8.5 Gy immediately before use. Twelve days later, their spleens were removed, fixed in Bouin's solution and scored for the presence of spleen colonies using an inverted microscope. For each donor, a minimum of five recipients was used.

For the CFU-E (erythroid colony forming unit) assays, bone marrow cells were mixed with Methocult M3334 (StemCell Technologies, Vancouver, BC, Canada) according to the manufacturer's guide lines. Assays were plated in 35-mm culture dishes in duplicate. CFU-E was scored on day 2.

3. Results

3.1. *Effect of FLV inoculation on the survival of TBI-treated C3H mice*

Kitagawa *et al.* (2002) showed that a sublethal split dose (1.5 Gy × 2) of whole-body irradiation causes death of FLV-infected C3H mice. To examine whether an FLV inoculation had a similar effect on the survival of C3H mice after treatment with a single dose of TBI, C3H mice were irradiated with a sublethal dose of 3 Gy on day 7 after FLV inoculation. Almost all mice died between 2 and 3 weeks post-irradiation (figure 1). These mice exhibited severe atrophy of spleen and bone marrow, and leukopenia and anaemia in peripheral blood, but no diarrhoea. In the unirradiated group, the treatment of FLV inoculation alone induced marked splenomegaly and leukaemia in all of the mice, and they died between days 47 and 91 after sham irradiation (figure 1). When the irradiated mice after FLV infection were injected with normal bone marrow cells immediately after irradiation, they were rescued from acute lethality but finally died of leukaemia with a delayed onset of tumour development of about 100 days post-irradiation (data not shown). C3H mice treated with a

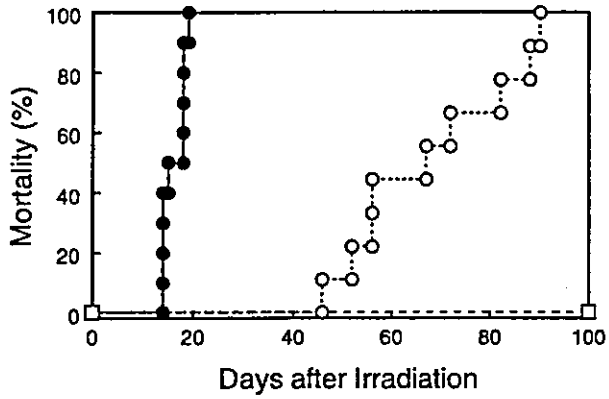

Figure 1. Mortality curve of C3H mice (n = 9) inoculated with FLV alone (open circles) or (n = 10) inoculated with FLV and, seven days later, treated with a sublethal dose (3 Gy) of irradiation (closed circles). Another group of C3H mice (n = 10) inoculated with FLV and irradiated was injected with 10^7 normal syngeneic bone marrow cells just after irradiation (open squares).

sublethal dose (3 Gy) of irradiation alone lived for more than 200 days.

3.2. *Strain difference in the enhancement effect of virus infection on radiation-induced mortality*

Kitagawa *et al.* (2002) showed that C3H mice treated with FLV alone died of leukaemia with splenomegaly from 4 to 8 weeks after irradiation, whereas C3H mice infected with FLV and treated with a sublethal split dose of irradiation (1.5 Gy × 2) died with severe atrophy of the spleen within 3 weeks after irradiation. We also observed that DBA/2 mice treated with FLV alone died of leukaemia with splenomegaly much faster than the C3H mice. In contrast to the case of C3H mice, the treatment with a split-dose of irradiation markedly extended the survival of FLV-infected DBA/2 mice.

To examine the effect of the genetic background of mice on the modifying effect by virus infection for radiation-induced mortality, FLV-sensitive strains of C3H, CBA/N and DBA/2 mice were examined. As shown in figure 2, C3H mice were the most sensitive strain, CBA/N mice were somewhat sensitive and DBA/2 mice were resistant. The mice of these FLV-sensitive strains surviving more than 30 days post-irradiation finally died of leukaemia. On the other hand, there was no mortality following the treatment with FLV inoculation and irradiation in the retro-virus-resistant strains of B10 and C4W mice, in spite of the fact that their resistance was controlled by different genes (B10: Fv-2^r, Fv-4^s; C4W: Fv-2^s, Fv-4^r) (data not shown).

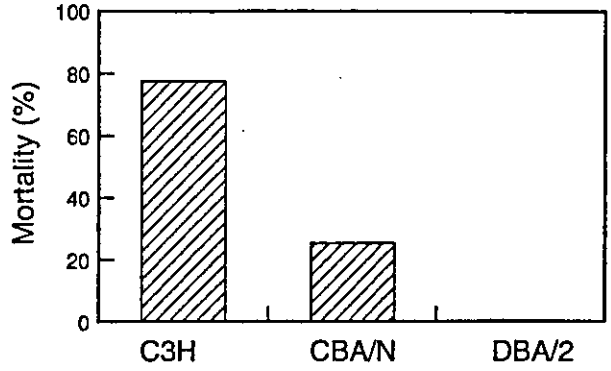

Figure 2. Strain differences in mortality of FLV-susceptible mice FLV-inoculated and treated with 3 Gy of irradiation at 7 days after FLV inoculation. Mortality was examined at 30 days after irradiation (n = 10 or 15 per group). Data represent mean ± SD (vertical lines) of mortality obtained from 4 (C3H), 2 (CBA/N) and 2 (DBA/2) experiments.

3.3. *Effect of radiation dose on mortality of virus-infected mice*

To examine the effect of radiation dose on mortality after a single dose of whole-body irradiation, mice were inoculated with FLV and irradiated at various doses 1 week later. As shown in figure 3, mice died with severe atrophy of spleen at 30 days after irradiation at doses of 1.5 Gy or higher in a dose-dependent manner. The mice surviving 30 days after irradiation died of leukaemia after 40 days post-irradiation.

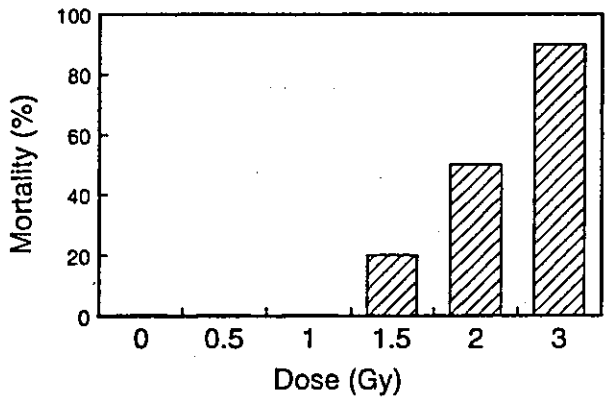

Figure 3. Effect of radiation dose on mortality of C3H mice inoculated with FLV and irradiated. Mortality was examined at 30 days post irradiation. Mice (n = 10 per group) were inoculated with FLV and, seven days later, treated with different doses (0.5–3.0 Gy) of irradiation.

3.4. *Effect of interval between virus inoculation and irradiation*

Various time intervals between FLV inoculation and irradiation (3 Gy) were used to determine the relationship, if any, between interval and enhanced radiation-induced mortality by virus infection. As shown in figure 4(a), only the mice irradiated at 1 week after virus inoculation exhibited high mortality, but the groups irradiated at 3 days or at more than 2 weeks did not. Similar results were obtained in the groups of mice irradiated at 2 Gy (data not shown). The phenomenon was reproducible when the mortality was examined in the groups of mice irradiated at three days, 1 and 2 weeks after virus inoculation. In an experiment with the groups of mice irradiated at days 4, 5, 6, 7, 8, 9 or 10 after virus inoculation (figure 4(b)), it was observed that the groups irradiated at day 5, 6 or 7 had high mortality, those irradiated at day 8 significant mortality, but those at day 4, 9 or 10 no mortality.

To investigate whether the resistance of DBA/2 mice was due to a shift in the time peak of sensitivity, the effect of time interval between FLV inoculation and irradiation on the mortality of DBA/2 mice was also examined. All mice in the groups with various time intervals survived for 30 days after irradiation and finally died of leukaemia (figure 4(c)).

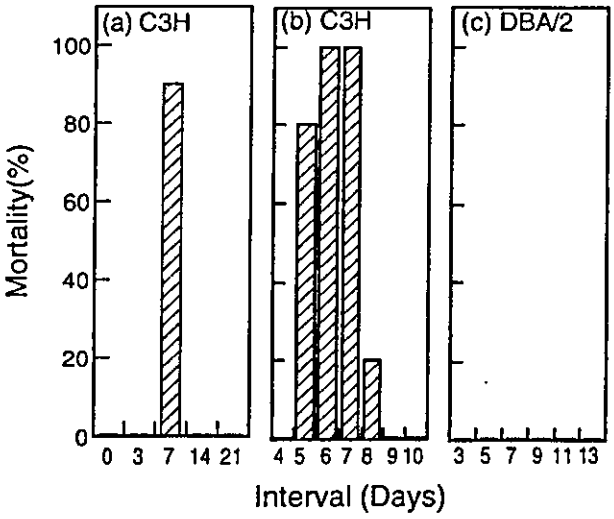

Figure 4. Effect of time interval between FLV inoculation and irradiation on mortality of C3H (a, b) and DBA/2 (c) mice. Mortality was examined at 30 days after 3 Gy of irradiation. Mice (n = 10 per group) were inoculated with FLV and treated with 3 Gy of irradiation at various days after FLV inoculation.

3.5. *Cellularity in peripheral blood, spleen and bone marrow of mice after virus inoculation and irradiation*

The observation of complete rescue with the transfer of normal bone marrow cells strongly suggested that acute mortality following the treatment with FLV inoculation and irradiation was due to haematopoietic failure (figure 1). To investigate further the cause of death in C3H mice that had been infected with FLV and irradiated 1 week later, cellularity in a variety of haematopoietic tissues of the mice was examined at 2 weeks after irradiation when they began to die. C3H mice treated with FLV inoculation and irradiation (FLV + IR group) manifested severe loss of cellularity in white blood cells (WBC) and platelets (PLT) in peripheral blood (figure 5) and in myeloid cells (Gr-1$^+$) and erythroid cells (TER$^+$) in bone marrow (figure 6), as compared with those of mice treated with either virus inoculation alone (FLV group) or irradiation alone (IR group). The number of red blood cells in the wasted and dying mice treated with FLV inoculation and irradiation was reduced to less than 20% of that of untreated normal C3H mice. On the other hand, the number of T (Thy1$^+$) and B (B220$^+$) lymphocytes in spleen of the C3H mice treated with FLV inoculation and irradiation was less than that of normal mice but almost the same as that observed in the irradiated-only group (figure 6). Intestinal tissues of the dying C3H mice 2 weeks after irradiation showed normal morphology, just as those of only-irradiated mice (data not shown). In addition, there was no significant abscessing macroscopically in liver and kidney tissues of dead animals. These results suggested that the severe loss of cellularity in peripheral

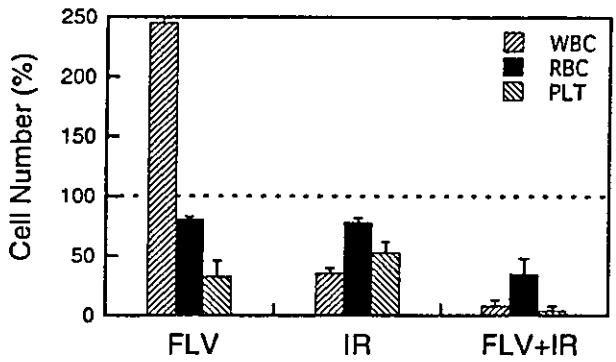

Figure 5. Number of white blood cells (WBC), red blood cells (RBC) and platelets (PLT) in peripheral blood of C3H mice two weeks after irradiation. Mice were treated with either FLV inoculation alone (FLV), irradiation alone (IR, 3 Gy), or FLV inoculation and, seven days later, irradiation (FLV+IR, 3 Gy). Data are shown as the percentage of values observed in untreated normal C3H mice used as control. Sample size was 6 mice in the FLV+IR group and 3 mice each in the other groups. Vertical bars represent SD.

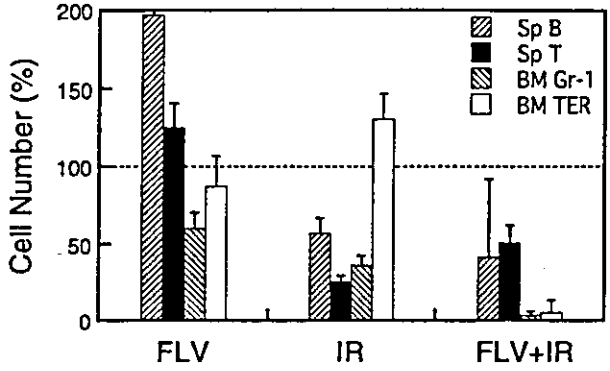

Figure 6. Numbers of Thy 1-positive spleen cells (Sp T), B220-positive spleen cells (Sp B), Gr-1-positive bone marrow cells (BM Gr-1) and TER-positive bone marrow cells (BM TER) of C3H mice two weeks after irradiation. Mice were treated with either FLV-inoculation alone (FLV), irradiation (IR, 3 Gy) alone, or FLV inoculation and, one week later, irradiation (FLV+IR, 3 Gy). Data are shown as the percentage of values observed in untreated normal C3H mice used as control. Sample size was 6 mice in the FLV+IR group and 3 mice each in the other groups. Vertical bars represent SD.

red blood cells might have been the main cause of death in C3H mice.

3.6. *Kinetics of peripheral blood cells in C3H mice irradiated at 1 and 2 weeks after FLV inoculation*

As shown in figure 3(a), only the group of mice irradiated at 1 week after virus inoculation exhibited a high rate of mortality, but the groups irradiated at three days and at more than 2 weeks after FLV inoculation did not. There was no significant change in the spleen weight of C3H mice 3 days after FLV inoculation. However, 2-fold and 4–5-fold increases in spleen weight were observed in the groups at 1 and 2 weeks post-FLV inoculation, respectively, accompanying a preferential increase in the number of TER-positive cells (data not shown). To characterize further the difference in mortality observed in the groups irradiated at 1 and 2 weeks after virus inoculation, we compared the kinetics of peripheral blood cells after irradiation (figure 7). The number of red blood cells (RBC) and white blood cells (WBC) in mice treated with irradiation alone decreased for ten days after irradiation and then began to increase, showing their regeneration. However, in the case of mice irradiated at 1 week after FLV inoculation, they continued to decrease without recovery. On the other hand, the group of mice irradiated at 2 weeks after FLV inoculation showed only about half the decrease in the number of RBC, and there was no significant decrease in WBC.

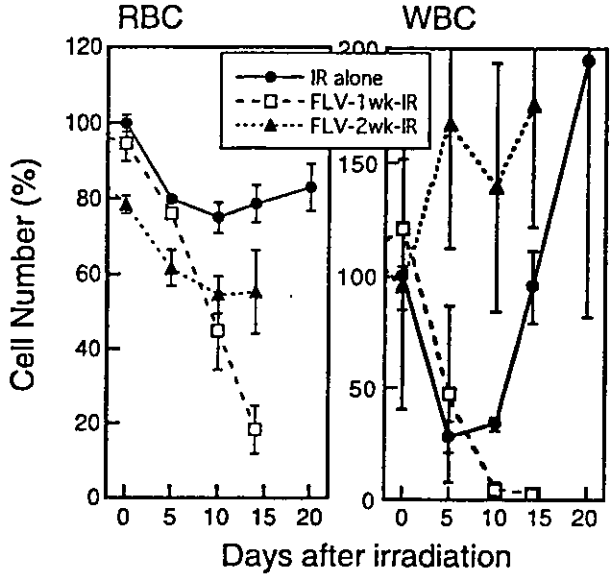

Figure 7. Kinetics of the numbers of peripheral red blood cells (RBC) and white blood cells (WBC) in C3H mice treated with FLV inoculation and irradiation. Mice (n=5 per group) were treated with irradiation (3 Gy) alone at day 0 (IR alone, closed circles), FLV inoculation at day -7 and, one week later, irradiation (FLV-1wk-IR, open squares), or FLV inoculation at day -14 and, two weeks later, irradiation (FLV-2wk-IR, closed triangles). Data are shown as the percentage of values observed in untreated normal C3H mice used as control. Vertical bars represent SD.

3.7. *Number and radiation sensitivity of haematopoietic stem cells in C3H mice infected with FLV*

The observation of leukopenia and anaemia in peripheral blood at 2 weeks post-irradiation in the group of mice irradiated at 1 week after FLV inoculation suggested that haematopoietic progenitor cells are also highly sensitive to the combined treatment of FLV infection and radiation. Therefore, to account for the difference in mortality of the mice irradiated at 1 and 2 weeks after virus inoculation (figure 3(a)), the number and radiosensitivity of CFU-S in bone marrow as a representative haematopoietic stem cell were examined in C3H mice at 1 and 2 weeks after FLV inoculation. The number of CFU-S in bone marrow of both groups of mice treated only with FLV inoculation decreased to less than half of those in untreated mice (-FLV group), but there was no significant difference between these two groups (figure 8(a)). Next, the radiation sensitivity of CFU-S was estimated from the number of CFU-S in bone marrow of C3H mice that were irradiated with 3 Gy at 1 or 2 weeks after FLV inoculation and maintained for one more week for the recovery of stem cells to a detectable level (figure 8(b)). The number of CFU-S

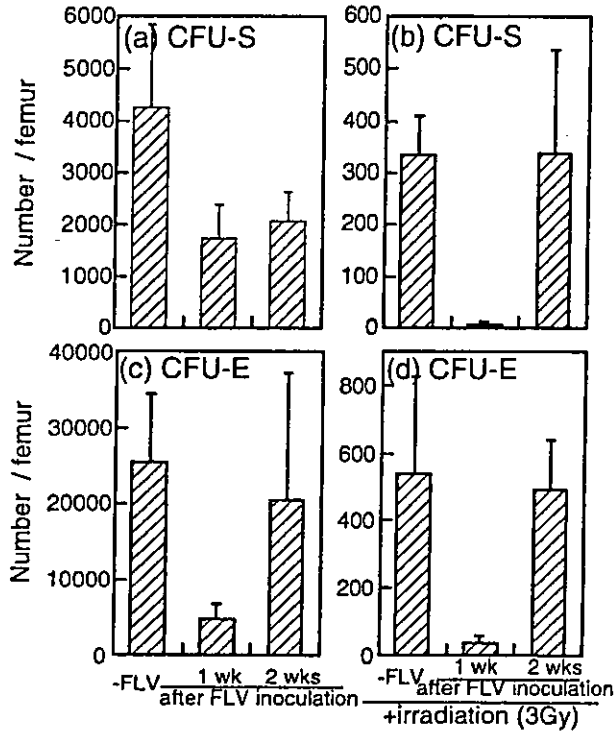

Figure 8. Number and radiation sensitivity of hematopoietic precursor cells (CFU-S and CFU-E) in bone marrow of C3H mice inoculated with FLV. The number of CFU-S was examined in bone marrow cells at one and two weeks after FLV inoculation (a) and the radiation sensitivity of CFU-S was estimated from the number of CFU-S in bone marrow cells of FLV-inoculated mice irradiated with 3 Gy one or two weeks after FLV inoculation and maintained one more week for stem cell recovery (b). Sample size: six bone marrow cells from each of 6 donor mice (a) and four donor bone marrow cells pooled from four or six donor mice in each group (b). Vertical bars represent SD.

The number of CFU-E was examined in bone marrow cells at one and two weeks after FLV inoculation (c) and the radiation sensitivity of CFU-E was estimated from the number of CFU-E in bone marrow cells taken out immediately after 3 Gy-irradiation one or two weeks post FLV inoculation (d). Sample size was six bone marrow cells from each of 6 donor mice (c, d) in each group. Vertical bars represent SD.

was greatly reduced in mice irradiated at 1 week after FLV inoculation, whereas that in mice irradiated at 2 weeks after FLV inoculation was almost the same as that in mice with irradiation only (-FLV group), highlighting the critically higher radiosensitivity of haematopoietic stem cells in mice 1 week post-FLV inoculation.

In addition, the number and radiosensitivity of CFU-E (erythroid colony forming unit) in bone marrow were also examined as precursor cells committed to peripheral RBC, since the severe loss of cellularity in peripheral RBC may be the main

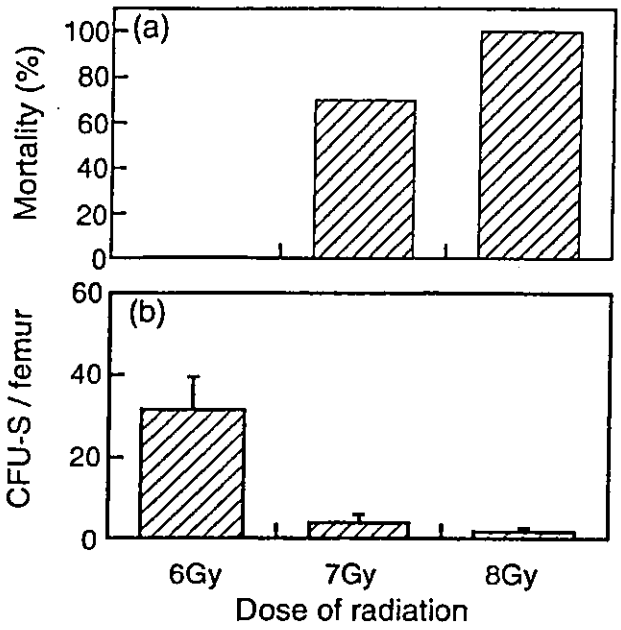

Figure 9. Mortality (a) and number of CFU-S (b) in C3H mice lethally irradiated. (a) Mortality was examined at 30 days post irradiation. Mice (n = 10 per group) were treated with different doses (6, 7, 8 Gy) of irradiation. (b) The number of CFU-S was examined in bone marrow cells at one week after irradiation. Sample size: three bone marrow cells pooled from 4 donor mice in each group. Vertical bars represent SD.

cause of death in C3H mice irradiated at 1 week after FLV inoculation. As shown in figure 8(c, d), the results were similar to those of CFU-S, indicating a higher radiosensitivity of CFU-E in mice 1 week post-FLV inoculation.

3.8. *Mortality and number of CFU-S in irradiated-only mice*

To demonstrate that the reduced level of CFU-S in mice irradiated at 1 week after FLV inoculation could not sustain life (figures 1 and 8), the relationship between mortality and the number of CFU-S was examined with mice treated with various doses of radiation alone. The mice with reduced levels of CFU-S observed in mice irradiated at 1 week after FLV inoculation had acute mortality (groups of 7 and 8 Gy in figure 9), while the mice with a 10-fold higher level of CFU-S (group of 6 Gy) did not show mortality, demonstrating the requirement of such a level of CFU-S to sustain life.

4. Discussion

The purpose of this study was primarily to characterize the cellular events in the enhancement

of radiation-induced haematopoietic injury by FLV infection. When C3H mice were treated with a sublethal dose (3 Gy) of irradiation at around 1 week after virus inoculation, most died around 15 days post-irradiation. Such combined procedures resulted in a severe loss of cellularity in haematopoietic tissues. However, this deleterious effect of virus infection on the survival of mice was only observed when they were irradiated at around 1 week after virus inoculation. Strain differences were also observed in the sensitivity to this effect even among virus-sensitive strains.

With regard to the strain difference in enhancement effect of FLV infection on radiation-induced mortality, C3H mice were the most sensitive strain, CBA/N mice were sensitive to a lesser degree and DBA/2 mice were resistant among the strains sensitive to FLV-induced leukaemogenesis. Since C3H and CBA/N inbred-strain mice were originally developed through a series of crosses between Bagg albinos and the DBA/2 strain (Strong 1942), CBA/N mice should be genetically much closer to C3H than DBA/2 mice. It has been shown that the degree of radiation-induced apoptosis in bone marrow of DBA/2 mice was almost the same as that in C3H mice (Kitagawa *et al.* 2002). However, differences in sensitivity to radiation-induced apoptosis became prominent in the FLV-infected groups of mice.

The present study demonstrated that FLV-infected C3H mice exhibited a marked loss of cellularity especially in erythroid (TER^+) and myeloid cells ($Gr\text{-}1^+$) in the bone marrow 2 weeks after irradiation, whereas uninfected C3H mice had a lesser degree of cellularity loss after irradiation, followed by regeneration. Kitagawa *et al.* (2002) reported that the bone marrow of C3H mice exposed to both FLV inoculation and irradiation showed a significant increase in apoptotic cells, peaking at 12 h post-irradiation, although the treatment with either FLV alone or a sublethal dose of irradiation alone induced minimal apoptosis in bone marrow cells. CFU-S and CFU-E in bone marrow as a representative haematopoietic stem cell and precursor cells committed to erythroid lineage, respectively, also became highly sensitive to radiation 1 week after FLV inoculation. Taken together, these results suggest that the decrease in the number of haematopoietic cells in C3H mice undergoing both FLV inoculation and irradiation was caused by a high level of radiation-induced apoptosis of not only haematopoietic lineage cells themselves, but also their progenitor cells.

In contrast to erythroid (TER^+) and myeloid cells ($Gr\text{-}1^+$) in bone marrow, there was no significant difference in the cellularity of splenic T- and B-lymphocytes 2 weeks after irradiation between C3H mice treated with irradiation alone and those treated with FLV inoculation and irradiation, showing no enhancing effect of virus infection on the radiation sensitivity of lymphocyte populations. On the other hand, as has been known for a long time (Bloom and Bloom 1954, Schrek 1961, Kataoka and Sado 1975), we also observed that splenic T- and B-lymphocytes were highly radiosensitive and their cell number quickly dropped to 30–40% of control in both groups of mice at the first day after the sublethal dose (3 Gy) of irradiation, irrespective of viral infection. Although it is not known why enhancement of radiosensitivity by FLV infection was not induced in lymphocyte populations, it has been shown that receptors for ecotropic murine leukaemia virus are also expressed on splenic T- and B-lymphocytes as well as TER^+ erythroid cells (Suzuki *et al.* 2001).

It is known that FLV infection inhibits various kinds of immune response in infected mice at early stages post-infection (Odaka *et al.* 1966, Mortensen *et al.* 1974). Thus, it is possible that the immunosuppression induced by FLV infection causes a reduced level of production of haematopoiesis-related cytokines like interleukins 2, 3, 4, 5 and 6, which might result in a lesser degree of haematopoiesis and a higher radiation sensitivity of haematopoiesis. However, the relationship between immunosuppression and haematopiesis itself is still controversial. Note that the *scid* (severe combined immunodeficiency) mutation specifically impairs lymphoid but not myeloid differentiation (Dorshkind *et al.* 1984), while interleukin 2-deficient mice develop a haematopoietic disorder characterized by anaemia and neutropenia (Reya *et al.* 1998). Thus, it has yet to be determined whether immunosuppression induced by FLV infection plays a critical role for enhancement of radiation-induced haematopoietic injury of C3H mice by FLV infection.

Mice exhibited severe mortality after the combined treatment with virus inoculation and a sublethal dose of irradiation, but it occurred only when the interval between virus inoculation and irradiation was 5, 6 and 7 days, not when it was shorter or longer (figure 4(b)). The lack of enhancement effect on the mortality of mice treated with irradiation at 3 days after FLV inoculation may be presumed to be due to an insufficient time for the spread of viral infection to a significant population of haematopoietic tissues. With regard to the absence of enhancement of radiosensitivity of haematopoiesis in the group of mice irradiated at 2 weeks after FLV inoculation, it has so far been reported that the total number of CFU-S increased by a factor of 10 in the spleen 2 weeks after virus infection and that the CFU-S probably remain multipotent and manifest radioprotective activity

(Okunewick *et al.* 1972, Okunewick and Phillips 1973). In addition, we observed a higher radiosensitivity of CFU-S and CFU-E in bone marrow of C3H mice 1 week after FLV inoculation as compared with that of CFU-S and CFU-E in bone marrow of normal mice and C3H mice 2 weeks after FLV inoculation (figure 8(b)). The difference in radiosensitivity of CFU-S between the mice 1 and 2 weeks after virus inoculation may significantly influence the regeneration of haematopoietic tissues after irradiation and lead to the fatal outcome of animals treated with a sublethal dose of irradiation after virus inoculation.

However, it is not known why there was a difference in radiation sensitivity of CFU-S and some haematopoietic lineage cells of C3H mice between 1 and 2 weeks after FLV inoculation. FLV infection usually causes anti-apoptotic features in transformed cell lines (Quang *et al.* 1997, Kelly *et al.* 1998, Pereira *et al.* 1999) as well in as primary erythroblasts (Quang *et al.* 1997). In contrast, Kitagawa *et al.* (2002) showed that FLV infection strongly enhances radiation-induced apoptotic cell death of haematopoietic cells, and that the apoptosis occurs through a p53-associated signalling pathway, because p53 knockout mice exhibited a very low frequency of apoptosis in bone marrow after FLV inoculation and irradiation. Daniel *et al.* (1999) reported that DNA-dependent kinase (DNA-PK)-deficient murine scid cells infected with retroviruses showed a substantial reduction in retroviral DNA integration and died by apoptosis, suggesting that the initial events in retroviral integration are detected as DNA damage by the host cells. Thus, the different state of viral genome in the amount of DNA double-stranded ends generated after viral infection might influence the radiation sensitivity of the host cells. However, it is clear that further study of the molecular mechanism responsible for the enhancement of radiation-induced apoptosis and mortality by FLV infection will be required to clarify the strain difference and time dependence of the enhancement of radiation-induced haematopoietic injury by FLV infection. It should also be noted that the evaluation of the molecular mechanism for the enhancement of radiation-induced apoptosis by virus infection is important for clarifying the significance of virus infection for radiation risk in a human population.

Acknowledgements

The authors thank the staff of the Animal Facility of National Institute of Radiological Science for the supply of clean mice and the maintenance of the animal facility, and Ms H. Arai for animal care. Work was in part supported by a grant from the Ministry of Education, Culture, Sports, Science and Technology of Japan.

References

Accornero, P., Radrizzani, M., Care, A., Mattia, G., Chiodoni, C., Kurrle, R. and Colombo, M. P., 1998, HIV/gp 120 and PMA/ionomycin induced apoptosis but not activation induced cell death require PKC for Fas-L upregulation. *FEBS Letters*, **436**, 461–465.

Bennett, L. R., Reckers, P. E. and Howland, J. W., 1951, The influence of infection on the hematological effects and mortality following mid-lethal X-radiation. USAEC Report UR-140. *Radiology*, **57**, 99–103.

Bloom, W. and Bloom, M. A., 1954, Histologic changes after irradiation. In A. Hollander (ed.), *Radiation Biology* (New York: McGraw-Hill), vol. 1, pp. 1091–1143.

Corbeil, J. and Richman, D. D., 1995, The role of surface CD4 in HIV-induced apoptosis. *Advances in Experimental and Medical Biology*, **374**, 91–99.

Daniel, R., Katz, R. A. and Skalka, A. M., 1999, A role for DNA-PK in retroviral DNA integration. *Science*, **284**, 644–647.

Dorshkind, K., Keller, G. M., Phillips, R. A., Miller, R. A., Bosma, G. C., O'Toole, M. and Bosma, M. J., 1984, Functional status of cells from lymphoid and myeloid tissues in mice with severe combined immunodeficiency disease. *Journal of Immunology*, **132**, 1804–1808.

Kataoka, Y. and Sado, T., 1975, The radiosensitivity of T- and B-lymphocytes in mice. *Immunology*, **29**, 121–130.

Kelly, L. L., Hicks, G. G., Hsieh, F. F., Prasher, J. M., Green, W. F., Miller, M. D., Eide, E. J. and Ruley, H. E., 1998, Endogenous p53 regulation and function in early stage Friend virus-induced tumor progression differs from that following DNA damage. *Oncogene*, **17**, 1119–1130.

Kitagawa, M., Aizawa, S., Kamisaku, H., Hirokawa, K. and Ikeda, H., 1999, Protection of retrovirus-induced disease by transplantation of bone marrow cells transduced with MuLV *env* gene via retrovirus vector. *Experimental Hematology*, **27**, 234–241.

Kitagawa, M., Matsubara, O. and Kasuga, T., 1986, Dynamics of lymphocytic subpopulations in Friend leukemia virus-induced leukemia. *Cancer Research*, **46**, 3034–3039.

Kitagawa, M., Yamaguchi, S., Hasegawa, M., Sado, T., Hirokawa, K. and Aizawa, S., 2002, Friend leukemia virus infection enhances DNA damage-induced apoptosis of hematopoietic cells, causing lethal anemia in C3H hosts. *Journal of Virology*, **76**, 7790–7798.

Korn, H. I. and Kallman, R. F., 1956, The influence of strain on acute X-ray lethality in the mouse. I. LD50 and death rate studies. *Radiation Research*, **5**, 309–317.

McLaughlin, M. M., Dacquisto, M. P., Jacobus, D. P. and Horowitz, R. E., 1964, Effects of the germfree state on responses of mice to whole-body irradiation. *Radiation Research*, **23**, 333–349.

Meinl, E., Fickenscher, H., Thome, M., Tschopp, J. and Fleckenstein, B., 1998, Anti-apoptotic strategies of lymphotropic viruses. *Immunology Today*, **19**, 474–479.

Miller, C. P., Hammond, C. W. and Tompkins, M., 1950, The incidence of bacteremia in mice subjected to total-body X-radiation. *Science*, **111**, 540–541.

Mori, N., Okumoto, M., Yonezawa, M., Nishikawa, R.,

TAKAMORI, Y. and ESAKI, K., 1994, Factors related to resistance to hematopoietic death in mice. *Journal of Radiation Research*, **35**, 1-10.

MORTENSEN, R., CEGLOWSKI, W. and FRIEDMAN, H., 1974, Leukemia virus-induced immnosuppression. X. Depression of T cell-mediated cytotoxicity after infection of mice with Friend leukemia virus. *Journal of Immunology*, **112**, 2077-2086.

ODAKA, T., ISHII, H., YAMAMURA, K. and YAMAMOTO, T., 1966, Inhibitory effect of Friend leukemia virus infection on the antibody formation to sheep erythrocytes in mice. *Japanese Journal of Experimental Medicine*, **36**, 277-290.

OKUNEWICK, J. P. and PHILLIPS, E., 1973, Changes in marrow and spleen CFU compartments following leukemia virus injection: comparison of Friend and Rauscher virus. *Blood*, **42**, 885-892.

OKUNEWICK, J. P., FULTON, D. and MARKOE, A. M., 1972, Radioprotective effect of Rauscher leukemia virus in the SJL/J mouse. *Radiation Research*, **49**, 521-529.

PEREIRA, R., QUANG, C. T., LESAULT, I., DOLZNIG, H., BEUG, H. and GHYSDAEL, J., 1999, FLI-1 inhibits differentiation and induces proliferation of primary erythroblasts. *Oncogene*, **18**, 1597-1608.

QUANG, C. T., WESSELY, O., PIRONIN, M., BEUG, H. and GHYSDAEL, J., 1997, Cooperation of Spi-1/PU.1 with an activated erythropoietin receptor inhibits apoptosis and Epo-dependent differentiation in primary erythroblasts and induces their Kit ligand-dependent proliferation. *EMBO Journal*, **16**, 5639-5653.

REYA, T., CONTRACTOR, N. V., COUZENS, M. S., WASIK, M. A., EMERSON, S. G. and CARDING, S. R., 1986, Abnormal myelocytic cell development in interleukin-2 (IL-2)-deficient mice: evidence for the involvement of IL-2 in myelopoiesis. *Blood*, **91**, 2935-2947.

SCHREK, R., 1961, Qualitative and quantitative reactions of lymphocytes to X-rays. *Annals of the New York Academy of Sciences*, **95**, 839-848.

SHEN, R. N., HORNBACK, N. B., LU, L., YOUNG, P., BRAHMI, Z. and BRONMEYER, H. E., 1988, Curative effect of split low dosage total-body irradiation on mice infected with the polycythemia-inducing strain of the Friend virus complex. *Cancer Research*, **48**, 2399-2403.

STRONG, L. C., 1942, The origin of some inbred mice. *Cancer Research*, **2**, 531-549.

SUZUKI, T., AIZAWA, S. and IKEDA, H., 2001, Expression of receptor for ecotropic murine leukemia virus on hematopoietic cells. *Archives of Virology*, **146**, 507-519.

TILL, J. E. and MCCULLOCH, E. A., 1961, A direct measurement of the radiation sensitivity of normal bone marrow cells. *Radiation Research*, **14**, 213-222.

UNSCEAR, 1982, *United Nations Scientific Committee on the Effects of Atomic Radiation Report* (New York: UN).

UNSCEAR, 2000, *United Nations Scientific Committee on the Effects of Atomic Radiation Report* (New York: UN).

VAN BEKKUM, D. W., 1991, Radiation sensitivity of the hematopoietic stem cell. *Radiation Research*, **128**, S4-S8.

YUHAS, J. M. and STORER, J. B., 1962, On mouse strain differences in radiation resistance: Hematopoietic death and the endogenous colony-forming unit. *Radiation Research*, **39**, 608-622.

Available online at www.sciencedirect.com
SCIENCE DIRECT®
Bioorganic & Medicinal Chemistry 13 (2005) 265–275
Bioorganic & Medicinal Chemistry

Synthesis and biological relationships of 3′,6-substituted 2-phenyl-4-quinolone-3-carboxylic acid derivatives as antimitotic agents

Ya-Yun Lai,[a] Li-Jiau Huang,[a] Kuo-Hsiung Lee,[b] Zhiyan Xiao,[b] Kenneth F. Bastow,[b] Takao Yamori[c] and Sheng-Chu Kuo[a,*]

[a]*Graduate Institute of Pharmaceutical Chemistry, China Medical University, Taichung, Taiwan*
[b]*Natural Products Laboratory, School of Pharmacy, University of North Carolina, Chapel Hill, NC 27599, USA*
[c]*Division of Experimental Chemotherapy, Cancer Chemotherapy Cancer, Japanese Foundation for Cancer Research, Tokyo 170-8455, Japan*

Received 14 February 2004; accepted 21 September 2004
Available online 12 October 2004

Abstract—As part of a continuing search for potential anticancer drug candidates in the 2-phenyl-4-quinolone series, 3′,6-substituted 2-phenyl-4-quinolone-3-carboxylic acid derivatives and their salts were synthesized and evaluated. Preliminary screening showed that carboxylic acid analogs containing a *m*-fluoro substituted 2-phenyl group displayed the highest in vitro anticancer activity. Activity decreased significantly if a chlorine or methoxy group replaced the fluorine atom. 3′-Fluoro-6-methoxy-2-phenyl-4-quinolone-3-carboxylic acid (**68**) had the highest in vitro cytotoxic activity among all tested carboxylic acid derivatives and their salts. The mechanism of action may be similar, but not identical, to that of tubulin binding drugs, such as navelbine and taxol. Compound **68** merits further investigation as a novel hydrophilic antimitotic agent.

1. Introduction

Quinolone derivatives were initially discovered as bacterial DNA gyrase inhibitors, and thus, developed as antibacterial agents.[1–5] Recently, DNA topoisomerase II has emerged as the pharmacological target for this class of quinolone compounds.[6–14] In our prior studies, substituted 2-phenyl-4-quinolones (A) were identified as novel antimitotic agents,[15,16] and structure–activity relationships (SAR) were established with many related

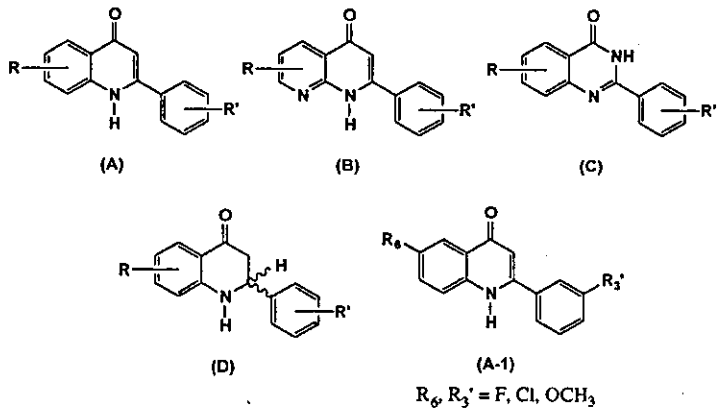

* Corresponding author. Fax: +886 4 2203 0760; e-mail: sckuo@mail.cmu.edu.tw

0968-0896/$ - see front matter © 2004 Elsevier Ltd. All rights reserved.
doi:10.1016/j.bmc.2004.09.041

synthetic analogs, including 2-phenylnaphthyridine-4-ones (B),[17] 2-phenyl-4-quinazolones (C),[18,19] and tetrahydro-2-phenyl-4-quinolones (D).[20] Among these analogs, many compounds, including 3′,6-disubstituted 2-phenyl-4-quinolones (A-1),[21] possessed potent cytotoxic activity against human tumor cell lines. However, most of these compounds were quite lipophilic, and therefore, not optimal for in vivo and clinical studies. Introducing a carboxylic acid group into the 2-phenyl-4-quinolone skeletone should increase polarity and might improve the pharmacokinetic properties of this cytotoxic compound class.

The design of target compounds was based on comparative Molecular Force Field (CoMFA) models derived from 104 known colchicine binding site antimitotic agents, including thiocolchicines, quinolones, and naphthyridinones,[22] and catalyst common-feature pharmacophore models, which were generated from 10 structurally diverse, colchicine binding site agents.[23] A closer examination of these pharmacophore models indicated that substitution at the 3-position did not interfere with any molecular area that is critical for antimitotic activity. Therefore, the antimitotic activities of 3-substituted and unsubstituted 2-phenyl-4-quinolones should be similar, and the effects of different phenyl substituents should also be comparable (3′,6-electron-rich substitution is favored in the parent series). Based on this hypothesis, 3′,6-substituted 2-phenyl-4-quinolone-3-carboxylic acids (**61–71**) and their salts (**72–82**) were designed as potential hydrophilic antimitotic agents. In this paper, the synthesis and in vitro cytotoxic activities of novel derivatives of 2-phenyl-4-quinolone with improved hydrophilicity are described.

2. Results and discussion

2.1. Chemistry

The synthesis of the key intermediates, ethyl 3′,6-disubstituted 2-phenyl-4-quinolone-3-carboxylates (**46–56**), is illustrated in Scheme 1.[24] Reaction of *p*-substituted anilines (**1–3**) with *m*-substituted benzoyl chlorides (**4–7**) yielded the corresponding *N*-(*p*-substituted phenyl)-3-substituted benzamides (**8–18**). Subsequent chlorination of compounds **8–18** with PCl_5 afforded carboximidoyl chlorides **19–29**, which, without further purification, were then treated with sodium diethylmalonate (**30**) to give the corresponding *N*-[1-(3-substituted phenyl)-2-diethoxycarbonylvinyl]-*N*-(4-substituted phenyl) amines (**31–41**).

These intermediates (**31–41**) were thermally cyclized to the corresponding ethyl 3′,6-disubstituted 2-phenyl-4-quinolone-3-carboxylates (**46–56**). During the purification of products **46**, **47**, **48**, and **51**, the 3′,6-disubstituted 2-phenyl-4-quinolones (**57–60**) were also obtained. Therefore, mono-ethoxycarbonyl vinyl derivatives (**42–45**) might have also been produced during the preparation of intermediates **31**, **32**, **33**, and **36**. Indeed, the mono-ethoxycarbonyl vinyl derivative (**42**) could be isolated and thermally cyclized to 3′-chloro-6-fluoro-2-phenyl-4-quinolone (**57**).

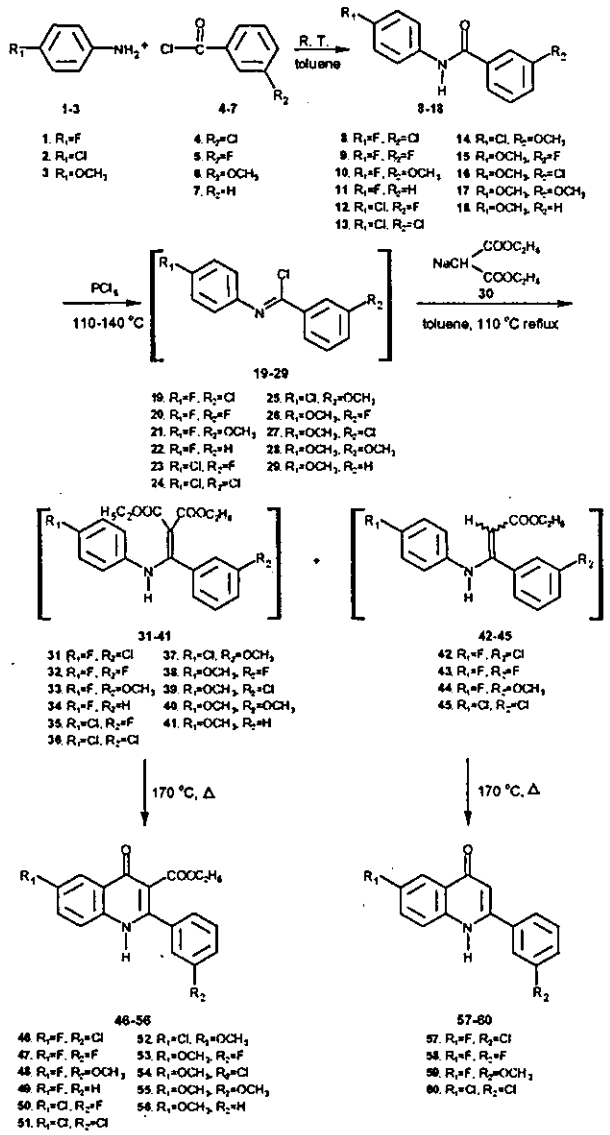

Scheme 1.

The synthetic route from key intermediates **46–56** to the target compounds **61–82** is illustrated in Scheme 2. As shown, compounds **46–56** were first hydrolyzed to the carboxylic acids (**61–71**), which were subsequently treated with tromethamine to afford the corresponding salts (**72–82**).

2.2. In vitro cytotoxic activity

Initial screening was performed using the human lung cancer (A549) cell line. As shown in Table 1, the tested ethyl esters (**50**, **52–55**) were inactive. Among the tested 3-carboxylic acid derivatives (**61–71**), only compounds **62**, **65**, and **68**, which contain a fluorine atom at the *m*-position of the 2-phenyl group, showed significant activity.

3′-Fluoro-6-methoxy-2-phenyl-4-quinolone-3-carboxylic acid (**68**) was the most potent compound with an

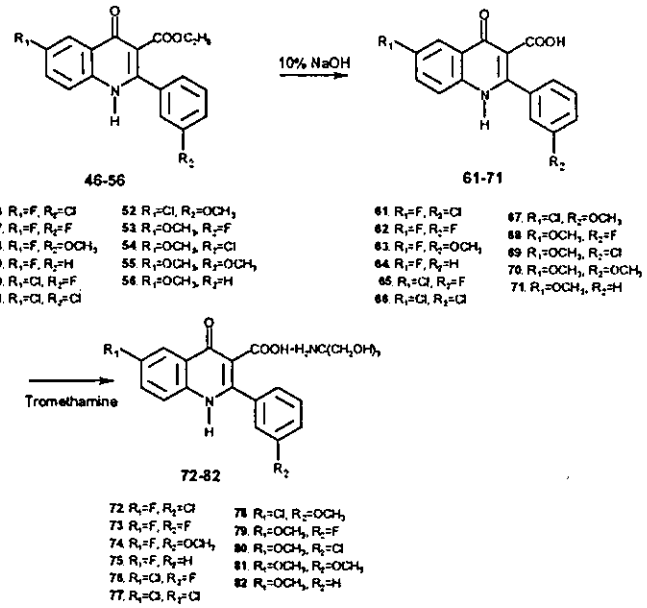

Scheme 2.

Table 1. Cytotoxicity data for compounds 50, 52–55, 61–63, and 65–71 against A549 lung cancer cells

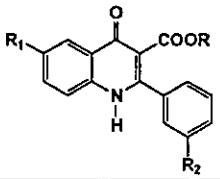

Compd	R	R_1	R_2	ED_{50} (μg/mL)[a]
50	CH_2CH_3	Cl	F	>20
52	CH_2CH_3	Cl	OCH_3	>20
53	CH_2CH_3	OCH_3	F	NA
54	CH_2CH_3	OCH_3	Cl	>20
55	CH_2CH_3	OCH_3	OCH_3	>20
61	H	F	Cl	20
62	H	F	F	0.5
63	H	F	OCH_3	>20
65	H	Cl	F	1.80
66	H	Cl	Cl	>20
67	H	Cl	OCH_3	>20
68	H	OCH_3	F	0.19
69	H	OCH_3	Cl	20
70	H	OCH_3	OCH_3	>20
71	H	OCH_3	H	>20

[a] Cytotoxicity expressed as ED_{50} against A549 (the concentration of compounds that causes a 50% reduction in absorbance at 562nm relative to untreated cells using the SRB assay).[22]

Table 2. Cytotoxicity data for compounds 72–74 and 76–82 against A549 lung cancer cells

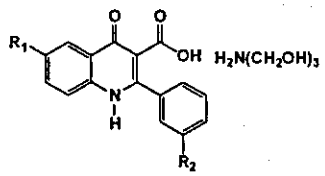

Compd	R_1	R_2	ED_{50} (μg/mL)[a]
72	F	Cl	17.6
73	F	F	4.3
74	F	OCH_3	NA
76	Cl	F	10.9
77	Cl	Cl	>20
78	Cl	OCH_3	>20
79	OCH_3	F	2.4
80	OCH_3	Cl	17.6
81	OCH_3	OCH_3	NA
82	OCH_3	H	>20

[a] Cytotoxicity expressed as ED_{50} against A549 (the concentration of compounds that causes a 50% reduction in absorbance at 562nm relative to untreated cells using the SRB assay).

ED_{50} of 0.19 μg/mL. Activity decreased ($ED_{50} \geqslant 20$ μg/mL) when the *m*-position of the 2-phenyl group was substituted with OCH_3 (**63**, **67**, and **70**), Cl (**61**, **66**, and **69**), or H (**71**) rather than F.

The cytotoxic activity data for the tromethamine salts are presented in Table 2. The potencies followed the general order: 3′-fluoro-derivatives (**73**, **76**, and **79**) ≫ 3′-chloro-derivatives (**72**, **77**, and **80**) > 3′-methoxy derivatives (**74**, **78**, and **81**). Similarly with the carboxylic acids, the salt (**79**) of compound **68** showed the best in vitro cytotoxic activity with an ED_{50} of 2.4 μg/mL.

The in vitro cytotoxic activity of compounds **68** and **79** was further tested in eight additional cancer cell lines (CAKI, HOS, KB, KB-VIN, SK-MEL-2, U87-MG, HCT-8, and IA9). As shown in Table 3, these two compounds demonstrated marked inhibition against most of

Table 3. Activity of compounds 68 and 79 against HTCL replication

Compd	ED_{50} (μg/mL)[a]							
	CAKI[b]	HOS[b]	KB[b]	KB-VIN[b]	SK-MEL-2[b]	U87-MG[b]	HCT-8[b]	1A9[b]
68	10.0	0.14	0.13	0.13	0.16	1.50	0.14	0.03
79	NT	5.0	NT	NT	2.0	5.0	1.20	0.88

[a] Cell line/mean ED_{50} in microgram per milliliter (duplicates varied no more than 5%). Note: if inhibition is less than 50% at 10 μg/mL then inhibition values observed are shown in brackets. NT = not tested.

[b] Renal cancer (CAKI), bone (HOS), epidermoid carcinoma of the nasopharynx (KB), vincristine-resistant epidermoid carcinoma of the nasopharynx (KB-VIN), melanoma (SK-MEL-2), glioblastoma (C187-MG), ileocecal carcinoma (HCT-8), human ovarian cancer (1A9) cell lines.

the eight cancer cell lines, and most notably, were quite active against human ovarian cancer cells (1A9), which are known to have a high level of drug resistant P-glycoprotein. Compound 68 showed an ED_{50} of 0.03 μg/mL against 1A9 cells, and also was equally active against vincristine-sensitive and -resistant KB cells. Thus, this compound merits further anticancer development, particularly against drug resistant ovarian cancer and vincristine-resistant epidermal carcinoma of the nasopharynx.

Based on the excellent preliminary results, compound 68 was further evaluated against the JCI human cancer cell line panel,[25] which includes five breast cancer, six CNS, five colon, seven lung, one melanoma, five ovarian, two renal, six stomach, and two prostate cancer cell lines. Dose response curves at five different concentrations between 10^{-4} and 10^{-8} M, which were obtained from computer analysis. GI_{50} (50% growth inhibition), TGI (total growth inhibition), and LC_{50} (50% lethal concentration) were calculated and the corresponding mean graphs (fingerprints) obtained.

Compound 68 was active against most cancer cell lines, with a MG-MID (mean growth midpoint) for $\log GI_{50}$ of −6.22. The highest potency was found against HGC2998 cells ($\log GI_{50}$ −6.86), followed by OVCAR-4 ($\log GI_{50}$ −6.76) cells. When evaluated for TGI (Table 2B), compound 68 had a mean log value of −4.61, with marked inhibition against BSY-1 breast, SF-539 CNS, HGC2998 colon, NCI-H552 lung, OVCAR-4 and SK-OV-3 ovarian, RXF-631L renal, and DU-145 prostate cancer cell lines. The mean log value for the LC_{50} values was −4.05. Compound 68 showed impressive selective toxicity against the OVCAR-4 cell line with $\log LC_{50}$ value of −6.02, which is 100-fold different in comparison to the mean value. Therefore, compound 68 is an excellent lead compound and worthy of further development.

Most drugs with the same mechanism of action will show similar fingerprints against a cancer cell line database. Therefore, the fingerprint of compound 68 was submitted for data analysis by a computer pattern recognition (COMPARE) program, which has a database covering fingerprints of over 100 known anticancer agents with various action mechanisms. The three highest correlation coefficient (r) values that were statistically significant ($p < 0.05$) are presented in Table 4. Compound 68 was closest to navelbine ($r = 0.521$), followed by vindesine ($r = 0.461$), and then taxol ($r = 0.452$),

Table 4. Results of COMPARE analysis of compound 68

Rank	Compd	r[a]	Molecular targets/drug type
1	Navelbine	0.512	Tubulin
2	Vindesine	0.461	Tubulin
3	Taxol	0.452	Tubulin

[a] r: correlation coefficient.

which suggests that 68 shares a similar action mechanism with these drugs. A possible mechanism is tubulin binding and subsequent inhibition of microtubule organization. However, to prove this possibility, the tubulin binding activity of 68 must be examined. Compound 68 may have a different mode of action compared to the above tubulin binders, as the correlation coefficients were low. Further investigation is required to clarify the action mechanism of this novel compound.

3. Conclusions

In order to improve the pharmacokinetic properties of antimitotic 2-phenyl-4-quinolone derivatives, molecular modeling was used to design a series of 3-carboxylic acid analogs. Initial cytotoxicity screening in the A549 cancer cell line identified 3′-fluoro-6-methoxy-2-phenyl-4-quinolone-3-carboxylic acid (68) as the most active compound. In further in vitro cytotoxic evaluation, this compound showed impressive potency against OVCAR-4 cancer cells. Analysis by the COMPARE program suggested a similar, but not identical, mechanism of action to that of navelbine and taxol. Compound 68 is an attractive candidate for development as a novel anticancer agent.

4. Experimental

Melting points were determined on a Yanaco MP-500D melting point apparatus and are uncorrected. IR spectra were recorded on Shimadzu IR-440 and Nicolet Impact 400 FT-IR spectrophotometers as KBr pellets. NMR spectra were obtained on a Bruker Advance DPX-200 FT-NMR spectrometer in DMSO-d_6 The following abbreviations are used: s, singlet; d, doublet; t, triplet; q, quartet; m, multiplet; and br, broad. MS spectra were measured with an HP 5995 GC–MS instrument. The UV spectra were recorded on a Shimadzu UV-160A UV–vis recording spectrophotometer as methanolic solutions. Elemental analyses (C, H, N) were performed